For a comparison reaction, 8 mL of ICH_2CH_3 (0.1 mmol) was added to 0.8 mL of D_2O in a 5-mm NMR tube. After the solution was allowed to stand at room temperature for 2 days, the ^1H-NMR spectra indicated that ICH_2CH_3 was the only species in the solution.

Acknowledgment. This research was funded by grants from the National Science Foundation (CHE-8906587) and the U.S. Department of Energy, Office of Basic Energy Sciences (DE-FG02-84ER13295). We thank Johnson Matthey, Inc. for a generous loan of platinum salts.

Registry No. THF, 109-99-9; K_2PtCl_4, 10025-99-7; Pt, 7440-06-4; O_2, 7782-44-7; $DO(CH_2)_3CO_2D$, 141981-61-5; CH_3COOD, 758-12-3; $DO(CH_2)_2OD$, 2219-52-5; $K[PtCl_3(CH_2{=}CH_2)]$, 12012-50-9; Na_2PtCl_6, 16923-58-3; K_2PtCl_6, 16921-30-5; $CH_3(CH_2)_2OD$, 4712-36-1; $DO(CH_2)_3OD$, 58161-12-9; $CH_3CH_2CO_2D$, 21388-62-5; HCO_2D, 925-94-0; CH_3COCH_3, 67-64-1; $K[PtCl_3(CH_2{=}CHCH_3)]$, 12075-59-1; $CH_3CO_2CH_2CH_3$, 141-78-6; $CH_3CH_2OCH_2CH_2OCH_2CH_3$, 629-14-1; CH_3CHO, 75-07-0; $OCHCH_2OCH_2CH_3$, 22056-82-2; $CH_3CH_2(OCH_2CH_2)_2OCH_2CH_3$, 112-36-7; $CH_3O(CH_2CH_2O)_4CH_3$, 143-24-8; $OCHCH_2O(CH_2CH_2O)_3CH_3$, 141981-62-6; CH_3CH_2OH, 64-17-5; $HOCH_2CH_2OH$, 107-21-1; $DOCH_2COOD$, 81278-02-6; $ClCH_2COOD$, 1837-59-8; CH_3CH_2OD, 925-93-9; $Cl(CH_2)_2OD$, 14848-86-3; CO, 630-08-0; $CH_3CH(OD)CH_3$, 3979-51-9; ICH_2CH_3, 75-03-6; $K_2[PtCl_5(CH_2CH_3)]$, 141981-63-7; H_2O, 7732-18-5; ethane, 74-84-0; propane, 74-98-6; γ-butyrolactone, 96-48-0; diethyl ether, 60-29-7; acetic acid, 64-19-7; di-*n*-propyl ether, 111-43-3; diisopropyl ether, 108-20-3; propylene, 115-07-1.

Homogeneous Catalysis: A Ruthenium-Based Lewis-Acid Catalyst for the Diels–Alder Reaction

William Odenkirk,[†] Arnold L. Rheingold,[‡] and B. Bosnich*,[†]

Contribution from the Department of Chemistry, 5735 South Ellis Avenue, The University of Chicago, Chicago, Illinois 60637, and Department of Chemistry and Biochemistry, The University of Delaware, Newark, Delaware 19716. *Received February 18, 1992*

Abstract: In order to circumvent some of the inherent drawbacks of using traditional Lewis acids to catalyze the Diels–Alder and other Lewis-acid-promoted reactions, a ruthenium-based catalyst has been devised. The readily prepared catalyst is *trans*-$[Ru(salen)(NO)(H_2O)]SbF_6$, where salen is the *N*,*N*′-bis(salicylidene)ethylenediamine dianion ligand. It has been fully characterized; it is stable to oxygen and can be handled under normal laboratory conditions. At 1 mol % loadings, the catalyst accelerates Diels–Alder reactions by many orders of magnitude over the corresponding thermal reaction. In many cases, accelerations of $>10^5$ are observed. The catalysis proceeds even in the presence of water. Slight product inhibition is observed, but the catalyst will continue to turn over substrates indefinitely. The binding of the Diels–Alder adduct of methacrolein and isoprene with the catalyst has been examined. Binding of the dienophile is stronger than that of the adduct. It is found that binding of the dienophile is endoergic, exchange of the aquo ligand is rapid and reversible, and a competitive equilibrium exists between the aquo species and the dienophile adduct. Overall, the catalyst is a mild Lewis acid which promotes Diels–Alder reactions of aldehyde and ketone dienophiles but not of α,β-unsaturated esters. Its mild Lewis-acid characteristics, however, serve to suppress polymerization even with sensitive substrates.

The classical Diels–Alder reactions involving, among others, α,β-unsaturated aldehydes, ketones, and 1,3-dienes are known to be promoted by Brønsted[1] and Lewis acids.[2] Moreover, the Lewis-acid-induced transformations always lead to higher stereoselectivities than do the corresponding thermal reactions. The most commonly used Lewis acids are the lighter halides of tervalent boron and tetravalent titanium and tin. For reasons which we discuss presently, these species are generally employed in stoichiometric or greater proportions. Even when the Lewis acids are used at catalytic levels, the loadings are generally high, of the order of 20 mol %. Many of these catalytic species have been modified by incorporation of chiral ligands. Although these modifications lead to less active Lewis acids, they are capable of engaging in enantioselective transformations. Remarkably high enantiomeric excesses have been obtained, generally at low temperatures, for the classical and hetero Diels–Alder reactions.[3] As a practical matter, these successes represent important achievements but attempts to understand the mechanisms of catalysis and selectivity present a formidable challenge because of the complexity of the chemical behavior of these modified Lewis acids. Consequently, the design of these modified chiral catalysts is largely dependent on intuition and on untested suppositions about the origins of the selection. It is for these reasons that we have searched for less complicated Lewis-acid systems. This is the first in a series of papers which attempts to circumvent the intrinsic problems associated with the use of classical Lewis acids for enantioselective catalysis. We describe a Lewis-acid catalyst derived from a transition metal which has many unique characteristics, including its potential rational modification into an asymmetric catalyst.

General Considerations

The traditional Lewis acids, BX_3, AlX_3, TiX_4, and SnX_4, have a number of undesirable or inconvenient characteristics. Among these is, first, their extreme sensitivity to water, which is one of the reasons that they are generally employed at high catalytic loadings. Second, binding between traditional Lewis acids and the oxygen atoms of the dienophile and of the product is generally thermodynamically strong, and in some cases exchange may be

[†] The University of Chicago.
[‡] The University of Delaware.

(1) Wassermann, A. *J. Chem. Soc.* **1942**, 618.
(2) (a) Yates, P.; Eaton, P. *J. Am. Chem. Soc.* **1960**, *82*, 4436. (b) Fray, G. I.; Robinson, R. *J. Am. Chem. Soc.* **1961**, *83*, 249. (c) Lutz, E. F.; Bailey, G. M. *J. Am. Chem. Soc.* **1964**, *86*, 3899. (d) Inukai, T.; Kasai, M. *J. Org. Chem.* **1965**, *30*, 3567. (e) Inukai, T.; Kojima, T. *J. Org. Chem.* **1966**, *31*, 1121. (f) Oppolzer, W.; Chapuis, C. *Tetrahedron Lett.* **1983**, *24*, 4665. (g) Masamune, S.; Reed, L. A.; Davis, J. T.; Choy, W. *J. Org. Chem.* **1983**, *48*, 4441.
(3) (a) Hashimoto, S.; Komeshima, N.; Koga, K. *J. Chem. Soc., Chem. Commun.* **1979**, 437. (b) Kelly, T. R.; Whiting, A.; Chandrakumar, N. S. *J. Am. Chem. Soc.* **1986**, *108*, 3510. (c) Narasaka, K.; Inoue, M.; Okada, N. *Chem. Lett.* **1986**, 1109. (d) Narasaka, K.; Iwasawa, N.; Inoue, M.; Yamada, T.; Nakashima, M.; Sugimori, J. *J. Am. Chem. Soc.* **1989**, *111*, 5340. (e) Furuta, K.; Shimizu, S.; Miwa, Y.; Yamamoto, H. *J. Org. Chem.* **1989**, *54*, 1481. (f) Corey, E. J.; Imwinkelried, R.; Pikul, S.; Xiang, Y. *J. Am. Chem. Soc.* **1989**, *111*, 5493. (g) Rebiere, F.; Riant, O.; Kagan, H. B. *Tetrahedron: Asymmetry* **1990**, *1*, 199. (h) Kaufmann, D.; Boese, R. *Angew. Chem., Int. Ed. Engl.* **1990**, *29*, 545.

0002-7863/92/1514-6392$03.00/0

kinetically slow. Thus, under catalytic conditions, the turnover frequency decreases as the number of turnovers increases due to product binding (product inhibition). This problem can be overcome by employing large loadings of catalyst. Third, the catalysts BF_3, $AlCl_3$, and $TiCl_4$ are powerful Lewis acids which are capable of polymerizing or otherwise destroying substrates. When the conventional Lewis acids are modified by incorporation of ligands, the complexity associated with the catalysis is increased. Not only are the original features of water sensitivity, product inhibition, and side reactions maintained but additional problems arise. The catalysts are almost always generated in situ. From the point of view of understanding the process, there are a variety of problems that are associated with this approach. First, it is not always clear which species are produced. Second, since the parent halide is nearly always more active than the species incorporating the ligand, small amounts of the starting halide could be responsible for a major part of the catalysis. This, of course, would lead to a reduction in the overall enantioselection because of the achiral pathway. Similarly, if more than one ligated species is catalytically active, the selectivity will depend on the relative rates of the competing paths. Third, even if the ligated catalyst is isolated and purified, upon dissolution the traditional Lewis acids are known to form oligomers and to engage in ligand exchange depending on the nature of the ligand and the Lewis-acid element. Thus even with purification, the use of modified traditional Lewis acids presents a challenge in identifying the catalytic species.

Ideally a chiral Lewis-acid catalyst should have the following characteristics. First, the catalyst should accelerate the reaction by at least 100-fold over the thermal reaction at reasonable catalyst loadings so that the achiral thermal path essentially does not contribute to the transformation. It, however, cannot be so active as to induce polymerization or otherwise destroy the substrates. Thus the window of activity is defined by the rate of the thermal reaction and the rates of polymerization or destruction of the substrates. Second, for convenient handling, the catalyst should be insensitive to oxygen and should not be destroyed or have its catalytic activity strongly inhibited by the presence of small amounts of water. Third, in order to facilitate mechanistic understanding, a single well-defined species should exist under catalytic conditions. Fourth, the catalyst should have a fixed, stable geometry so that the origins of the enantioselection can be defined. Fifth, the catalyst should bind the dienophile oxygen atom or other binding functionality rapidly and reversibly. Sixth, the catalyst should not bind olefins; otherwise, such binding will inhibit catalysis. Seventh, the ligands should be easily modified to maximize the catalytic activity and selectivity.

Conventional Lewis acids are unlikely to meet these criteria, and we turned to transition metal based Lewis acids for species which might circumvent the inherent problems of traditional Lewis acids. This is largely an uncharted area with few guiding principles although the literature provides some hints about which metal and ligand combinations to choose.[4]

Selection of Catalyst

To some extent we were guided in our choice of the Lewis-acid catalyst by recent reports on the reactivities of the following four species: $[W(CO)_3(PR_3)(NO)(SbF_6)]$,[5] where the NO^+ and SbF_6^- ligands are trans to each other; $[Ru(Cp)(PPh_3)_2(CH_2{=}CH_2)]PF_6$[6] and $[HC(py)_3M(NO)_2](SbF_6)_2$,[7] where M = Mo or W and $HC(py)_3$ is tris(2-pyridyl)methane. $[W(CO)_3(PR_3)(NO)(SbF_6)]$ was found to be a powerful catalyst for classical Diels–Alder reactions, but it suffered from two serious disadvantages. First, the species is so "hot" that it causes polymerization of both the diene and dienophile. This polymerization can be the major reaction, depending on the Diels–Alder partners. Second, we have briefly investigated the effect of replacing the CO ligands with phosphine ligands and have found that, consistent with previous work,[5] successive incorporation of phosphines leads to a diminution of Lewis-acid activity. No detectable activity remains after three phosphines are added. Two conclusions may be drawn from these observations: first, as expected, soft ligands such as phosphines decrease Lewis acidity and, second, modification of this species into an effective enantioselective catalyst is made difficult because of the restricted amount of elaboration that can be performed. The $[Ru(Cp)(PR_3)_2(CH_2{=}CH_2)]PF_6$ species incorporates a basic ruthenium atom, which tends to prefer olefin to dienophile carbonyl coordination. Thus this complex does not promote the classical Diels–Alder reaction, and this aspect is not circumvented by replacing one of the phosphines by a carbonyl ligand.[8] Even so the $[Ru(Cp)(PPh_3)_2(CH_2{=}CH_2)]PF_6$ species is a useful catalyst for the less Lewis-acid-demanding hetero Diels–Alder (Danishefsky) reaction. In this case, the ethylene is replaced by the aldehyde during catalysis; when a chiral (bidentate) phosphine is incorporated, the ruthenium catalyst gives reasonable enantioselection for the hetero Diels–Alder reaction.[8]

The $[HC(py)_3M(NO)_2](SbF_6)_2$ (M = Mo, W) species were found to bind strongly to aldehydes, ketones, and esters and were found to promote the classical Diels–Alder reactions. When less basic dienophiles (esters) were used, however, considerable polymerization of the diene was observed.

From the above observations, we may draw a number of guidelines for the synthesis of transition metal Lewis acids. First, a spin-paired d^6 system is preferred because such systems generally form stable, stereochemically rigid octahedral complexes. The alternative is to consider oxophilic metals, which generally contain less than six d electrons. Our results on d^0 systems will be reported shortly. Second, if a d^6 system is chosen, the Lewis acidity will be enhanced by the presence of at least one electron-withdrawing NO^+ ligand and the presence of at least one overall positive charge on the complex. An investigation of the infrared data of nitrosyl complexes[9] suggests that Lewis acidity will be manifest if the NO^+ stretching frequency is around or greater than 1800 cm^{-1}. Third, the complex should have a real or virtual (labile ligand) vacant coordination position which can bind to a carbonyl oxygen group of a substrate. Probably, this vacant coordination position should be trans to the NO^+ ligand. Fourth, soft ligands, such as triaryl- or trialkylphosphines, should be avoided, since the incorporation of such ligands will tend to quench the Lewis acidity. Hard, weakly basic ligands or electron-withdrawing π-acids, such as the carbonyl ligand, will enhance Lewis acidity. These criteria narrow the possible metals and ligands that can be used if spin-paired d^6 systems are chosen. Guided by these principles, we decided to investigate complexes of the type *trans*-[Ru(salen)(NO)L]X, where L and X are weakly coordinating or noncoordinating ligands and salen is the *N,N'*-bis(salicylidene)ethylenediamine dianion.

Catalyst Synthesis

The catalyst precursor [Ru(salen)(NO)Cl] was prepared in acceptable yield (~50%) by the reaction of the disodium salt of salen and commercial $Ru(NO)Cl_3{\cdot}H_2O$ in DMF solution at 110 °C (eq 1). The product crystallizes as air-stable deep red-brown

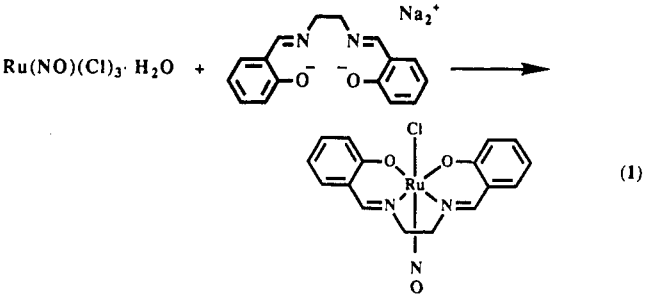

(1)

(4) Beck, W.; Sünkel, K. *Chem. Rev.* **1988**, *88*, 1405.
(5) (a) Hersh, W. H. *J. Am. Chem. Soc.* **1985**, *107*, 4599. (b) Honeychuck, R. V.; Bonnesen, P. V.; Farahi, J.; Hersh, W. H. *J. Org. Chem.* **1987**, *52*, 5293. (c) Bonnesen, P. V.; Puckett, C. L.; Honeychuck, R. V.; Hersh, W. H. *J. Am. Chem. Soc.* **1989**, *111*, 6070.
(6) Faller, J. W.; Smart, C. J. *Tetrahedron Lett.* **1989**, *30*, 1189.
(7) Faller, J. W.; Ma, Y. *J. Am. Chem. Soc.* **1991**, *113*, 1579.
(8) Faller, J. W.; Ma, Y.; Smart, C. J.; DiVerdi, M. J. *J. Organomet. Chem.* **1991**, *420*, 237.
(9) Connelly, N. G. *Inorg. Chim. Acta, Rev.* **1972**, *6*, 47.

Table I. Crystallographic Data for $[Ru(salen)(NO)(H_2O)]^+SbF_6^-\cdot 2C_3H_6O$

		(a) Crystal Parameters	
formula	$C_{22}H_{28}F_6N_3O_6RuSb$	γ, deg	105.48 (3)
fw	767.29	V, Å^3	1440.8 (11)
cryst syst	triclinic	Z	2
space group	$P\bar{1}$	cryst dimens, mm	0.26 × 0.27 × 0.38
a, Å	9.684 (4)	cryst color	dark red
b, Å	12.332 (6)	D(calc), g cm^{-3}	1.769
c, Å	12.705 (4)	μ(Mo Kα), cm^{-1}	15.3
α, deg	99.01 (3)	temp, K	295
β, deg	91.45 (3)	T(max)/T(min)	1.423
		(b) Data Collection	
diffractometer	Nicolet R3m	no. of indpt rflns	6566
monochromator	graphite	R(merg), %	2.7
radiation (λ, Å)	Mo Kα (0.71073)	no. of indpt obsvd rflns, $F_o \geq 4\sigma(F_o)$	4372
2θ scan range, deg	4–55	std rflns	3 std/197 rflns
no. of rflns collected	6854	var in stds	~30%
		(c) Refinement	
$R(F)$, %	6.31	$\Delta(\rho)$, e Å^{-3}	1.27
$R_w(F)$, %	6.93	N_o/N_v	12.4
Δ/σ(max)	0.02	GOF	1.389

crystals, which have a NO stretching frequency of 1828 cm^{-1}. This frequency suggests a highly electron-deficient metal center.[9] The ^{1}H NMR spectrum indicates that the chloro and nitrosyl ligands are trans disposed (see Experimental Section).

The [Ru(salen)(NO)Cl] species in acetone/dichloromethane solutions is readily dechlorinated by 1 equiv of silver salts, AgX, where X is the weakly coordinating anions PF_6^-, SbF_6^-, $CF_3SO_3^-$, and BF_4^-. In all cases, the isolated product, $[Ru(salen)(NO)(H_2O)]X$, has a coordinated aquo group. Addition of excess $NaBPh_4$ to a methanol solution of $[Ru(salen)(NO)(H_2O)]SbF_6$ gave the species $[Ru(salen)(NO)(H_2O)]BPh_4$. All of these species act as catalysts for the Diels–Alder reaction, despite their poor solubility in dichloromethane and limited solubility in nitromethane, the solvents used for catalysis. We found that the SbF_6^- salt possessed the most favorable characteristics for catalysis, and it was used throughout. As expected, the infrared stretching frequency of the NO^+ ligand in the aquo complexes increases over that of the neutral chloro analogs to 1889 cm^{-1}. In nitromethane solution, the $[Ru(salen)(NO)(H_2O)]SbF_6$ species is a 1:1 electrolyte (81 Ω^{-1} mol^{-1} cm^2; see Experimental Section) and, moreover, the ^{19}F NMR spectrum shows fluorine signals in regions found for free SbF_6^-. Thus we conclude that, in nitromethane solutions, the SbF_6^- ion is not coordinated to the metal. The ^{1}H NMR spectrum of $[Ru(salen)(NO)(H_2O)]SbF_6$ confirms the trans structure.

The aquo ligand shows a complex ^{1}H NMR behavior in CD_3NO_2 solutions. In dry CD_3NO_2, a 0.027 M solution of the aquo complex shows a ^{1}H NMR signal at $\delta \sim 2$, corresponding to free water, and two broad, overlapping signals of unequal intensity at around δ 8 at 25 °C, which we ascribe to bound water. The integrated intensities of the bound- and free-water proton signals are roughly equal. On cooling, both bound- and free-water signals shift downfield and become sharper. At all temperatures (+25 to −25 °C) the protons of the salen ligand remain sharp and only one set of signals is observed. Moreover, addition of 4 equiv of H_2O (10% ^{17}O) to the solution leads to the observation of one $^{17}OH_2$ signal in the ^{17}O NMR spectrum shifted downfield by 1.3 ppm from the signal for free water and shifted further downfield to 6.0 ppm upon cooling to −28 °C. All of these observations are consistent with a rapid equilibrium of the kind shown in eq 2. This

$$[Ru(salen)(NO)(H_2O)]^+ + CD_3NO_2 \rightleftharpoons [Ru(salen)(NO)(CD_3NO_2)]^+ + H_2O \quad (2)$$

equilibrium is shifted to the left upon addition of water, but the addition causes broadening of the bound- and free-water proton signals. Addition of 1 equiv of CF_3COOH also causes broadening of the bound-water proton signals. Thus it appears that, in addition to rapid water exchange, there is rapid proton exchange of the bound-water protons. We have been unable to unravel the details of the proton exchange, but the important observation that water exchange is rapid and reversible is secure.

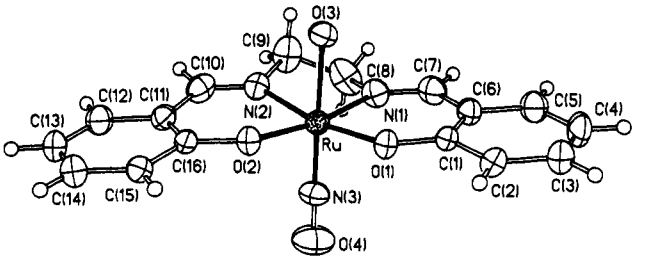

Figure 1. X-ray diffraction determined structure of $[Ru(salen)(NO)(H_2O)]^+$. Selected bond lengths (Å): Ru–O(1), 2.020 (4); Ru–O(2), 2.034 (5); Ru–O(3), 2.059 (5); Ru–N(1), 2.000 (6); Ru–N(2), 2.039 (5); Ru–N(3), 1.718 (7). Selected bond angles (deg): O(1)–Ru–(O)(2), 88.7 (2); O(1)–Ru–O(3), 83.8 (2); O(1)–Ru–N(1), 94.5 (2); O(1)–Ru–N(2), 169.2 (2); O(1)–Ru–N(3), 94.5 (2); O(2)–Ru–O(3), 85.8 (2); O(2)–Ru–N(1), 171.2 (2); O(2)–Ru–N(2), 92.8 (2); O(2)–Ru–N(3), 94.1 (3); O(3)–Ru–N(1), 86.4 (2); O(3)–Ru–N(2), 85.6 (2); O(3)–Ru–N(3), 178.3 (2); N(1)–Ru–N(2), 82.6 (2); N(1)–Ru–N(3), 93.8 (3); N(2)–Ru–N(3), 96.2 (3).

Despite the lability of the water ligand, we were unable to remove it by heating the solid complex at 80 °C under high vacuum for 24 h nor was it removed by use of 3-Å molecular sieves in nitromethane solutions. Attempts to obtain a methyl vinyl ketone adduct from a neat methyl vinyl ketone solution of the aquo complex led to the precipitation of the aquo complex upon the addition of hexane.

Structure of Catalyst

The crystal structure of the catalyst $[Ru(salen)(NO)(H_2O)]SbF_6\cdot 2(acetone)$ was determined by X-ray diffraction. The molecule crystallizes with two molecules of acetone in the crystal and, upon exposure, effloresces to a powder containing no acetone. The data were collected with the crystal in its mother liquid. Table I contains the X-ray data, and Figure 1 shows the structure. Selected bond lengths and angles are provided in the caption, and others are found in the supplementary material. Overall, the structure is unexceptional and is as expected, but we note a number of features. First, the Ru–N(3)–O(4) angle is 176.3° and the N(3)–O(4) bond length is 1.142 Å, which is consistent with a NO^+ ligand.[9] Second, the ethylenediamine ring is in a (chiral) puckered conformation, which would lead to the magnetic nonequivalence of the imine and aromatic protons in the ^{1}H NMR spectrum. The fact that these protons are found to be equivalent suggests that the molecule is undergoing conformational interconversion on the NMR time scale.

Diels–Alder Catalysis

The catalyst $[Ru(salen)(NO)(H_2O)]SbF_6$ is stable in air and can be handled normally without diminution in activity over

Table II. Diels–Alder Catalysis by $[Ru(salen)(NO)(H_2O)]SbF_6$ in CD_3NO_2 Solutions at 25 °C

	Dienophile	Diene	Time For 90 % Reaction (Hours)	Isomer Ratio	Major Product	Thermal: Time for 90 % Reaction[g] (Hours)	Thermal: Isomer Ratio
1			71	91 : 9	 [b]	3000	70 : 30
2			22	99 : 1	ND	$> 10^5$	93 : 7 [h]
3		 [a]	40	—	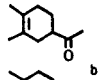	2000	—
4			5	99 : 1	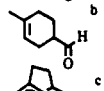 [b]	2700	70 : 30
5			4.4	98 : 2	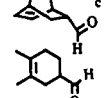 [c]	$> 10^5$	89 : 11 [h]
6		 [a]	3.3	—		2000	—
7			3	93 : 7	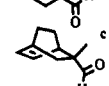 [d]	$> 10^5$	72 : 28 [h]
8			48	70 : 30	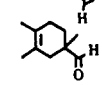 [c]	$> 10^5$	ND
9		 [a]	3.2	—	 [d]	14000	—
10			2	90 : 10	 [e]	300	86 : 14
11			718	92 : 8	ND	$> 10^5$	ND
12			70	92 : 8	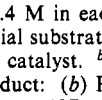 [f]	$> 10^5$	ND

[a] Initial substrate concentration is 1.4 M in each substrate using 2 mol % catalyst. In all other cases, initial substrate concentrations are 2.8 M in each substrate using 1 mol % catalyst. [b-f] References for assignment (^1H NMR) of the major product: (*b*) Reference 5c; ND = not determined. (*c*) Geibel, K. *Chem. Ber.* **1970**, *103*, 1637. (*d*) Balwin, J. E.; Lusch, M. J. *J. Org. Chem.* **1979**, *44*, 1923. (*e*) Reference 3h. (*f*) Brun, C.; Jenner, G.; Deluzarche, A. *Bull. Soc. Chim. Fr.* **1972**, 2332. [g] Time calculated by extrapolation of a second-order plot of the thermal reaction under the same concentrations of substrate used in catalysis at 25 °C. [h] Ratios obtained by heating substrates either neat or in CD_3NO_2 solution.

indefinite periods. We found that nitromethane was the most convenient solvent for catalysis although slower catalysis occurs in dichloromethane, in which the catalyst is poorly soluble, and in acetone. Acetonitrile solvent inhibited catalysis presumably because of coordination.

In general, the Diels–Alder reactions were conducted using a catalyst loading of 1 mol % and an initial concentration of the diene and dienophile of 2.8 M each. Thus the substrates constituted a large fraction of the initial solution. Catalysis proceeds equally well at lower initial concentrations. Some of our results are collected in Table II. In addition to the catalytic reactions, Table II contains the time the thermal reaction takes for 90% completion. The thermal reactions were measured under conditions identical to those used for the catalytic reactions. The times given were obtained by extrapolating a second-order plot of the reaction to 90% reaction. The times are approximate, but the orders of magnitude are correct. It will be noted that many of the thermal reactions could not be conveniently measured at 25 °C, and we estimate their rates as greater than 10^5 h. Apart from entries 1 and 3, the catalytic rate is many orders of magnitude faster than that of the thermal reaction, even at the very low catalyst loadings used. In all cases the catalytic rate can be increased by increasing the catalyst loading. As expected, the stereoselectivities for the catalytic reactions are greater than those for the traditional thermal reactions and the differences are comparable to those observed with traditional Lewis acids. Overall, this ruthenium-based catalyst is a milder catalyst than those derived from B^{3+}, Al^{3+}, and Ti^{4+}, but it has the advantage that no polymerization is observed for any of the substrates. Even acrolein is not polymerized by the present catalyst. The mildness of the catalyst is evidenced by the fact that no Diels–Alder catalysis is observed with methyl acrylate and dienes isoprene and cyclopentadiene. Generally the order of Diels–Alder reactivity is as follows: aldehydes are "faster" than ketones and esters are inactive. An important feature of the catalyst, however, is the absence of strong product inhibition. Since the substrate concentrations in Table II are high and cause volume changes, we investigated product inhibition at lower substrate concentrations to obviate the effects due to volume changes. Thus using 5.3 mol % catalyst in CD_3NO_2 at 25 °C, the catalyzed reaction of methacrolein (0.49 M) and isoprene (0.49 M) was 90% complete in 4.4 h. After no more substrate remained, more methacrolein (0.49 M) and isoprene (0.49 M) were added to the catalytic solution in the presence of product; 7.5 h was required for 90% completion of the reaction. Thus, although product inhibition appears to be real, it is not strong. The rate of a classical Diels–Alder reaction is dependent on the dienophile–catalyst binding constant, and if the product also binds to the catalyst, the product will inhibit the catalytic rate. The mildness of the product inhibition suggests that the binding constant is less for the product than for the dienophile. This difference is probably due to the greater steric hindrance of the product. That the binding is sensitive to steric effects is suggested by the observation that the catalytic reaction of methyl vinyl ketone and isoprene (entry 1) is at least 5 times faster than the reaction using ethyl vinyl ketone as a dienophile.

A unique feature of the present catalyst is its tolerance of water. Thus the catalytic rate of the partners shown in entry 7 was diminished by less than a factor of 2 by using nitromethane saturated with water (2% w/w) instead of dry nitromethane. As a practical matter, the catalysis can be conducted with commercial solvents without special precautions.

Aquo complexes of transition metals are generally mildly acidic, and it is conceivable that at least part of the catalysis is due to proton activation of the dienophile. We have checked the effect of acid on the reaction of methyl vinyl ketone and isoprene (entry 1) and also the reaction of acrolein and 1,3-cyclohexadiene (entry 5). Using the same concentrations of substrates as in catalysis and 1 mol % acetic acid ($pK_a = 4.75$) in CD_3NO_2 solution, no catalysis or decomposition is observed after 50 h for either pair of substrates. Using the much more powerful acid trifluoroacetic acid ($pK_a = 0.3$) under the same conditions caused slow proton catalysis in both cases, but for the methyl vinyl ketone–isoprene reaction, the proton-catalyzed reaction was 13 times slower than the ruthenium-catalyzed reaction and 150 times slower than the ruthenium-catalyzed reaction of acrolein and 1,3-cyclohexadiene. The selectivities for the proton and ruthenium catalysts are similar.

We note that the pK_a of the tricationic ruthenium aquo complex $[Ru(NH_3)_5(H_2O)]^{3+}$ is 4.2[10] and it is highly improbable that the present monocationic catalyst is any more acidic. Thus the proton activity of trifluoroacetic acid is likely to be many orders of magnitude greater than that of the catalyst, which is likely to be comparable to that of acetic acid, which casues no proton-induced Diels–Alder reaction. We conclude that the preponderant, if not sole, path for the catalysis is Lewis-acid association with the catalyst.

Adduct Formation

We have studied the formation of the adduct between methacrolein (MA) and the catalyst in dry CD_3NO_2. Because of the difficulties in obtaining completely dry CD_3NO_2 required for the low concentrations of catalyst used (0.027 M) and because of the problems of obtaining sufficiently accurate integrations of the ^1H NMR signals, we were unable to obtain accurate equilibrium constants for adduct formation. The overall quantitative behavior, however, has been ascertained.

Successive additions of methacrolein to a 0.027 M solution of $[Ru(salen)(NO)(H_2O)]SbF_6$ in distilled CD_3NO_2 solution led to

(10) Broomhead, J. A.; Basolo, F.; Pearson, R. G. *Inorg. Chem.* **1964**, *3*, 826.

the appearance of new ^1H NMR signals in the imine proton, the aromatic proton, and also the aldehyde proton regions of the spectrum. The new aromatic proton signals overlap with those of the adduct-free catalyst, but the signals of those protons associated with the aldehyde and imine groups are well separated at 500 MHz. The free-aldehyde proton signal occurs at δ 9.49, and the signal of the proton associated with the adduct occurs at δ 9.12. The signal of the unbound-catalyst imine proton occurs at δ 8.79 whereas the signal of this same proton in the adduct occurs at δ 8.73. The relative proportions of the aldehyde peaks and the relative proportions of the imine peaks indicate that substrate binding is responsible for the appearance of the new peaks. As more methacrolein is added, the adduct peaks steadily increase until 20 equiv is present. Addition of more aldehyde causes only minor increases in the adduct signal intensity. Consistently, the bound-water signal steadily decreases in intensity as more aldehyde is added up to 20 equiv. At these catalytic concentrations of the complex, it appears that the maximum binding is obtained at around 20 equiv of aldehyde. The ratio of free complex to adduct complex at 20 equiv of aldehyde is about 2:1 at 25 °C.

It is perhaps surprising that as the temperature is raised to 65 °C with 20 equiv of aldehyde present, the proportion changes so that at 65 °C the ratio of adduct to free complex is 1:1. Thus adduct formation appears to be an endoergic process, where more adduct is formed as the temperature is raised.

We have observed two types of mild catalytic inhibition, one due to the presence of water and the other due to the product. Accordingly, water should compete with adduct formation. This is so. Thus when water is successively added to a CD_3NO_2 solution of the catalyst and 20 equiv of methacrolein, the amount of adduct steadily diminishes, and after 6 equiv of water is added, only about 5% of the catalyst exists as the aldehyde adduct at 25 °C. The amount of adduct formed is very sensitive to the amount of water present, and as a result the determination of accurate equilibrium values was extremely difficult.

Using the product mixture obtained from the catalytic reaction of methacrolein and isoprene (entry 7), adduct formation was investigated under the previous conditions. Successive additions of this product mixture to the catalyst in CD_3NO_2 solution at 25 °C led to the appearance of new ^1H NMR signals in the aromatic regions. The new signal for the imine proton was very broad, suggesting rapid exchange. Using the integrated intensities of the aromatic proton resonances, we find that, after the addition of 20 equiv of the products, the amount of the adduct has approximately maximized. The ratio of catalyst to catalyst adduct is about 9:1. Thus the methacrolein substrate binds about 3 times more strongly than the Diels–Alder products derived from isoprene and methacrolein. The exceptionally mild product inhibition that is observed can be understood in these terms.

From these equilibrium studies, we conclude that the rate of Diels–Alder catalysis is governed by the existence of three equilibria (eqs 3–5) and by the rate of reaction of the dienophile–catalyst adduct with the diene. We have shown that the first equilibrium is established rapidly and reversibly on an NMR time scale, and we find that, in the other two cases (eqs 4 and 5), the equilibria are established upon mixing. Hence, the rate of catalysis is dependent not on the rates at which these equilibria are established but on the values of the equilibrium constants and the intrinsic rate.

$$[Ru(H_2O)]^+ + CD_3NO_2 \overset{K_1}{\rightleftharpoons} [Ru(CD_3NO_2)]^+ + H_2O \quad (3)$$

$$[Ru(H_2O)]^+ + \text{OHC-cyclohexene} \overset{K_2}{\rightleftharpoons} \left[\text{RuOHC-cyclohexene}\right]^+ + H_2O \quad (4)$$

$$[Ru(H_2O)]^+ + \text{OHC-cyclohexene} \overset{K_3}{\rightleftharpoons} \left[\text{RuOHC-cyclohexene}\right]^+ + H_2O \quad (5)$$

Discussion

The $[Ru(salen)(NO)(H_2O)]^+$ species is an effective Lewis–acid catalyst for the Diels–Alder reaction under low catalyst loadings of 1–2 mol %. For aldehyde- and ketone-bearing dienophiles, rate accelerations of over 10^5 are observed in many cases over the corresponding thermal reactions at these low catalyst loadings. Unlike previous d^6 transition metal based catalysts, the present catalyst does not cause polymerization of the substrates.

Perhaps the major interest of this work is that it describes a Diels–Alder catalyst which possesses most of the desirable properties which are difficult, if not impossible, to achieve with traditional Lewis acids. Thus, the catalyst can be handled without special precautions: it does not require dry solvents, it operates effectively under low catalyst loadings, its isolation and characterization are simple, catalysis proceeds indefinitely with only mild product inhibition, and it is readily modified in a systematic and predictable manner. In addition to these characteristics, the present catalyst possesses other desirable features. The aquo ligand is very labile and exchanges rapidly and reversibly with itself and with the dienophile. It is probable that rapid exchange is due, in part, to the presence of a trans-disposed NO^+ ligand. Despite the fact that water and the dienophile compete for binding to the catalyst, catalysis proceeds even in the presence of water although at a slower rate, as expected.

Overall, the present species is a mild Lewis-acid catalyst which is generally an excellent catalyst for aldehyde- and ketone-bearing dienophiles but which is ineffective for α,β-unsaturated esters. We suspect that this observation is an inevitable trade-off between our achieved suppression of polymerization of substrates and catalytic rate. This supposition is supported by the observation that although the $[W(CO)_3(PR_3)(NO)(SbF_6)]$[5] and the $[HC(py)_3W(NO)_2](SbF_6)_2$[7] species are more powerful Diels–Alder catalysts than our ruthenium complex, they are also powerful polymerization catalysts for 1,3-dienes. We have not observed 1,3-diene polymerization with the present catalyst.

It is possible that these ruthenium–salen catalysts will find application in reactions which require mild Lewis acids. Thus we have found that 1 mol % of $[Ru(salen)(NO)(H_2O)]SbF_6$ in CD_3NO_2 solution transforms *d*-citronellal to *l*-isopulegol in 80% yield in 4 h at 25 °C. This Prinz reaction has previously been accomplished with anhydrous zinc halides.[11] Similarly, we have found that the present catalyst is extremely effective for the Mukaiyama crossed aldol reaction. We shall report on this and related catalyzed transformations shortly.

Experimental Section

^1H NMR spectra were recorded on GE GN 500, GE QE 300, and The University of Chicago built 500-MHz spectrometers. Unless TMS is indicated, all ^1H NMR chemical shifts are reported relative to residual CHD_2NO_2 (^1H, δ 4.33), $CHDCl_2$ (^1H, δ 5.32), and C_6HD_5 (^1H, δ 7.15). The ^{19}F NMR spectrum was recorded on a Varian XL-400 spectrometer with $CFCl_3$ as an internal reference, and ^{17}O NMR spectra were obtained on the GE GN 500 spectrometer. Infrared spectra were obtained as mineral oil mull samples on NaCl plates on a Nicolet 20SXB FT-IR instrument. Conductivity measurements were performed using a Yellow Springs Instrument Model 35 conductance meter. Elemental analyses were performed by Desert Analytics, Tucson, AZ.

Solvents and reagents were obtained from Aldrich except for the following: $Ru(NO)Cl_3 \cdot H_2O$ (Strem); DMF, CH_2Cl_2, Et_2O, and CH_3NO_2 (Baker). $SalenH_2$ was prepared by a published procedure.[12] All

(11) Nakatani, Y.; Kawashima, K. *Synthesis* **1978**, 147.

substrates for catalysis were used as received except for methacrolein, which was vacuum-transferred from CaH_2 and stabilized with 0.01% hydroquinone, and 1,3-cyclohexadiene, which was vacuum-distilled from 3-Å molecular sieves.

[Ru(salen)(NO)(Cl)]. The following operations were carried out under argon. NaH (80% dispersion in mineral oil, 260 mg, 8.68 mmol) was weighed into a 200-mL Schlenk flask and washed with dry hexane (3 × 10 mL). Degassed DMF (30 mL) was added, followed by salenH_2 (1.05 g, 3.92 mmol), while the NaH suspension was rapidly stirred. Gas evolved (H_2), and the mixture was transformed into a clear yellow solution. After 20 min, $Ru(NO)(Cl)_3 \cdot H_2O$ (1.00 g, 3.92 mmol) was added, followed by more DMF (10 mL). The mixture was stirred at 110 °C for 22 h. An opaque red-brown mixture resulted, from which the DMF was removed under high vacuum (0.2 mm). From this point, all subsequent work was done in air. Methylene chloride (80 mL) and H_2O (90 mL) were added to the residue. The mixture was filtered through Celite. The filtrate was transferred to a 500-mL separatory funnel, and the two layers were separated. The dark red CH_2Cl_2 layer was washed with H_2O (3 × 80 mL). The CH_2Cl_2 layer was then stirred with anhydrous $MgSO_4$ (18 g) for 8 min, the mixture was filtered, and the filtrate volume was reduced under vacuum to 200 mL. The solution was treated again with more anhydrous $MgSO_4$ (14 g) by the same procedure. The volume of the final solution was reduced under vacuum to 30 mL, giving very fine dark red-maroon crystals. Slow addition of Et_2O precipitated more solid from the solution as well as a flocculent green side product. After the mixture was allowed to stand at 5 °C for 12 h, the crystals were filtered off and were then washed with Et_2O (30 mL), CH_2Cl_2/Et_2O (1:1, 25 mL), and finally cold CH_2Cl_2 (10 mL). The crystals were recrystallized twice more from CH_2Cl_2/Et_2O and were washed each time s ssively with CH_2Cl_2/Et_2O (1:1, 25 mL) and Et_2O (30 mL). The da rystals of [Ru(salen)(NO)(Cl)]·0.6CH_2Cl_2 (940 mg, 49% yield) obtained were air stable and were stored in a vacuum desiccator. The presence of CH_2Cl_2 in the crystals was confirmed by ^1H NMR spectroscopy. Heating a pulverized sample at 60 °C under high vacuum (0.2 mm) for 28 h resulted in the lowering of this ratio to 0.1 CH_2Cl_2 per unit of complex. This sample was used for elemental analysis. ^1H NMR (300 MHz, CD_3NO_2): δ 8.47 (s, 2 H, N=C*H*), 7.40–7.50 (m, 4 H, phenyl H), 7.04 (d, J = 8.4 Hz, 2 H, phenyl H), 6.70–6.76 (m, 2 H, phenyl H), 4.10–4.40 (m, 4 H, NCH_2CH_2N). IR (mull): ν(NO) 1828 cm^{-1}. Anal. Calcd for $C_{16}H_{14}N_3ClO_3Ru \cdot C_{0.1}H_{0.2}Cl_{0.2}$: C, 43.81; H, 3.24; N, 9.52; Cl, 9.64. Found: C, 43.77; H, 3.23; N, 9.31; Cl, 9.48.

[Ru(salen)(NO)(H_2O)]SbF_6. The [Ru(salen)(NO)(Cl)] complex contains variable amounts of CH_2Cl_2 in the crystal, depending on the length of storage. The amount should be determined by ^1H NMR spectroscopy before the following step. All steps were carried out under argon. To [Ru(salen)(NO)(Cl)]·0.26CH_2Cl_2 (248 mg, 0.54 mmol) in a 200-mL Schlenk flask, were added CH_2Cl_2 (20 mL) and acetone (15 mL). All but a small portion of the complex dissolved. A solution of $AgSbF_6$ (187 mg, 0.54 mmol) in acetone (20 mL) was then added via cannula, resulting initially in a dark red solution, which then became cloudy with precipitating AgCl. The flask was protected from light, and the reaction mixture was stirred for 1 h, after which it was gently heated to coagulate the AgCl. The mixture was then filtered through Celite into a 200-mL Schlenk flask, and the isolated solid was washed with acetone. The solvent was removed under vacuum, the residue was dissolved in acetone (50 mL), the resulting mixture was filtered through Celite, and the solvent was again removed under vacuum. The residue was dissolved once more in acetone (30 mL), and the resulting mixture was filtered through a 1.0-μm in-line filter into a 200-mL Schlenk flask. The solution volume was then reduced under vacuum to 10 mL, and the flask was suspended in an ice–water bath. Slow addition of hexane to the solution over 6 h gave dark red crystals. After the mixture was allowed to stand overnight at 0 °C, the crystals were filtered off and washed with hexane/acetone (10:2, 12 mL) and then hexane (15 mL). After a second crystallization from acetone/hexane, the dark red crystals were stored under argon for 1 day. The crystals originally obtained were dark red and transparent but rapidly lost solvent of crystallization (2 acetones per unit of complex) when stored under an inert atmosphere for 1 day. They became a rust red opaque solid, [Ru(salen)(NO)(H_2O)]SbF_6 (250 mg, 71% yield). This acetone-free solid was used in all further studies and analyses. The complex was stable in air and was routinely stored in a vacuum desiccator. ^1H NMR (300 MHz, CD_3NO_2): δ 8.79 (s, 2 H, N=C*H*), 7.80–8.30 (br unsym d, 1.4 H, Ru—OH_2), 7.49 (dd, J = 7.9, 1.6 Hz, 2 H, phenyl H), 7.00–7.15 (m, 2 H, phenyl H), 6.73–6.85 (m, 2 H, phenyl H), 6.47 (d, J = 8.41 Hz, 2 H, phenyl H), 4.30–4.70 (m, 4 H, NCH_2CH_2N), 2.10 (br s, H_2O, 0.8 H). ^{19}F NMR (400 MHz, CD_3NO_2, $CFCl_3$ internal reference: δ 122.15 (sextet, ^{121}Sb, $I = {}^5/_2$, J_{FSb} = 1931 Hz; octet, ^{123}Sb, $I = {}^7/_2$, J_{FSb} = 1014 Hz). IR (mull): ν(NO) 1889 cm^{-1}. Molar conductance (1×10^{-3} M solution in CH_3NO_2): Λ_M = 80.8 Ω^{-1} mol^{-1} cm^2 (1:1 electrolyte).[13] Anal. Calcd for $C_{16}H_{16}N_3O_4SbF_6Ru$: C, 29.51; H, 2.48; N, 6.45. Found: C, 29.82; H, 2.46; N, 6.47.

Diels–Alder Catalysis. In a typical procedure, [Ru(salen)(NO)(H_2O)]SbF_6 (9.2 mg, 14 μmol) was weighed into an NMR tube, which was then sealed with a rubber septum. Injection of CD_3NO_2 (266 μL) and acrolein (94 μL, 1.4 mmol) gave a dark red solution. Isoprene (140 μL, 1.4 mmol) was injected, and the catalysis was monitored by ^1H NMR spectroscopy. The product yields were determined by integration of product peaks against the substrate peaks. Data for products of the catalyses were compared with data for the thermal product and literature data where available. In all cases the selectivity observed in the thermal reaction was enhanced in the catalysis, with the same isomer being favored in both cases.

A large-scale catalysis was done as follows. [Ru(salen)(NO)(H_2O)]SbF_6 (18.4 mg, 28.3 μmol) was dissolved in CH_3NO_2 (625 μL) in a flask sealed with a rubber septum. Methacrolein (249 mg, 3.56 mmol) and isoprene (245 mg, 3.59 mmol) were then injected, and with stirring, the reaction went to completion in 12 h (^1H NMR). Benzene (9 mL) was then added, and the mixture was filtered and passed down a short Florisil column. The CH_3NO_2 was removed as the CH_3NO_2/benzene azeotrope, giving the product 1,4- and 1,3-dimethyl-3-cyclohexene-1-carboxaldehyde (1,4:1,3 = 95:5 by ^1H NMR spectroscopy) as a clear viscous oil (380 mg, 76%).

^{17}O NMR Study. [Ru(salen)(NO)(H_2O)]SbF_6 (9.46 mg, 14.5 μmol) was di: ' ed in dry CD_3NO_2 (514 μL) in an NMR tube sealed with a rubber um. Upon addition of H_2O (10 atom % ^{17}O, 0.54 μL, 2 equiv) at 25.0 °C to the complex solution, a peak at δ 1.44 appeared (referenced to $CD_3(^{17}O)NO$, δ 624.26). No other new peaks were seen. Further addition of H_2O (10 atom % ^{17}O, 0.54 μL, 2 equiv) caused a minor shift in this peak to δ 1.33. Cooling this latter solution to −28.0 °C caused a shift in the peak to δ 6.04. Warming to room temperature returned the spectrum to the original form.

Adduct Formation Studies. (a) Methacrolein Addition. [Ru(salen)(NO)(H_2O)]SbF_6 (27.9 mg, 42.9 μmol) was dissolved in dry CD_3NO_2 (1.53 mL) in an NMR tube sealed with a rubber septum. Four additions of methacrolein (MA) (115, 118, 198, 198 mg) were then made, to give a final solution containing 21 equiv of MA. ^1H NMR spectra were recorded after each new addition of MA, and a new set of peaks attributed to the adduct between the complex and MA appeared and grew in intensity as the concentration of MA was increased. Some sets of resonances due to the adduct and the free complex overlap. The ratio of adduct to free complex was calculated from the areas of the peaks of the imine hydrogens of the adduct (δ 8.73) and of the free complex (δ 8.79). This ratio was found to be 1.0:2.2 after the final addition of MA. That adduct formation was indeed being monitored was confirmed by the appearance of a new aldehyde proton signal (δ 9.12), which increased in intensity with increase in MA concentration.

A series of ^1H NMR spectra of the final solution from the MA addition study were acquired at the following temperatures: 25.0, 35.0, 45.0, 55.0, and 65.0 °C. As the temperature was raised, the ratio of the adduct species relative to the free complex increased and at 65.0 °C was 1.0:1.0. After the temperature was lowered to 25.0 °C, the adduct peaks and free complex peaks returned to their original intensities.

(b) Water Addition. [Ru(salen)(NO)(H_2O)]SbF_6 (27.6 mg, 42.5 μmol) was dissolved in dry CD_3NO_2 (1.57 mL) in an NMR tube sealed with a rubber septum. MA (63.3 mg, 903 μmol) was added. The ratio of adduct to free complex was 1.0:1.9 (^1H NMR). Three additions of D_2O (99.8 atom % D) were then made (1.70, 1.81, 1.81 mg) to give a total of 6.2 equiv of D_2O. The ratio of adduct to free complex decreases with each addition to a final value of 1.0:17.0.

(c) Diels–Alder Product Addition. [Ru(salen)(NO)(H_2O)]SbF_6 (9.30 mg, 14.3 μmol) was dissolved in dry CD_3NO_2 (505 μL) in an NMR tube sealed with a rubber septum. A mixture of the Diels–Alder product of methacrolein and isoprene, 1,4- and 1,3-dimethyl-3-cyclohexene-1-carboxaldehyde (where (1,4):(1,3) = 95:5), was added in four portions (10 mg × 4), and a ^1H NMR spectrum was acquired after each addition. The spectra showed very small broad peaks in the region associated with the imine hydrogen of the dienophile–complex adduct (δ 8.70–8.76) as well as in the phenyl region. After the final addition of product (20 equiv), the ratio of adduct to free complex was 1:9.

Prinz Reaction. [Ru(salen)(NO)(H_2O)]SbF_6 (1.7 mg, 2.6 μmol) was dissolved in CD_3NO_2 (467 μL) in an NMR tube sealed with a rubber septum. *d*-Citronellal (46 μL, 254 μmol) was injected, and the catalysis was monitored by ^1H NMR spectroscopy. The reaction went to 90% completion in 4 h. After the reaction had gone to completion (6 h), a

(12) Thornback, J. R.; Wilkinson, G. *J. Chem. Soc., Dalton Trans.* **1978**, 110.

(13) Geary, W. J. *Coord. Chem. Rev.* **1971**, *7*, 107.

sample (100 μL) of the catalysis solution was diluted with benzene (500 μL) and the precipitated catalyst was filtered off. Azeotropic distillation yielded a viscous oil, which was examined by ^{1}H NMR spectroscopy. All of the four possible cyclization products were observed in C_6D_6, and the major product (80%) was confirmed to be *l*-isopulegol by a ^{1}H NMR comparison with the reported spectrum.[11]

Crystal Structure. Preliminary photographic characterization revealed no symmetry higher than triclinic; this was later confirmed by TRACER. The centrosymmetric space group alternative was initially chosen statistically. The chemically reasonable bond parameters obtained from refinement suggested that this assignment was correct. A linear correlation for a 30% decay in the check reflection intensity during data collection (due to loss of acetone) and an empirical absorption correction were applied to the data.

An autointerpreted Patterson routine was used to locate the Ru and Sb atoms. All non-hydrogen atoms were refined anisotropically, and hydrogen atoms were treated as idealized, isotropic contributions. All computations used SHELXTL (version 5.1) software (G. Sheldrick, Nicolet (Siemens), Madison, WI).

Acknowledgment. This work was supported by grants from the National Institutes of Health.

Supplementary Material Available: Tables of bond distances, bond angles, atomic coordinates, and anisotropic/isotropic thermal parameters (7 pages); a listing of structure factors (13 pages). Ordering information is given on any current masthead page.

Ground Spin State Variability in Manganese Oxo Aggregates. Demonstration of an $S = {}^3/_2$ Ground State for $[Mn_3O_4(OH)(bpea)_3](ClO_4)_3$[1]

Samudranil Pal, Michael K. Chan, and William H. Armstrong*,†

Contribution from the Department of Chemistry, University of California, Berkeley, California 94720. *Received December 30, 1991*

Abstract: Synthesis and properties of bi- and trinuclear manganese oxo complexes of the ligand *N,N*-bis(2-pyridylmethyl)ethylamine (bpea) are reported. The binuclear species $[Mn_2O_2(O_2CCH_3)(bpea)_2](ClO_4)_3$ (**1**) was isolated in 41% yield from a MeOH reaction mixture that contained $Mn(O_2CCH_3)_3{\cdot}2H_2O$, bpea, and aqueous $HClO_4$. Compound **1** crystallizes from $CHCl_3$/CH_3CN/*n*-hexane as **1**·CH_3CN·0.5$CHCl_3$ in the triclinic space group $P\bar{1}$ with a = 12.956 (1) Å, b = 12.987 (2) Å, c = 13.391 (2) Å, α = 77.20 (1)°, β = 83.34 (1)°, γ = 80.36 (1)°, V = 2158.8 (6) Å^3, and Z = 2. Bond distances and angles for **1** are consistent with a Mn^{IV}_2 oxidation state assignment. The variable temperature magnetic susceptibility data for **1** in the range 6–280 K were fit with the expression generated from the isotropic spin Hamiltonian $\mathcal{H} = -2J\hat{S}_1{\cdot}\hat{S}_2$ ($S_1 = S_2 = {}^3/_2$), with J = −124 cm^{-1}. Compound **1** was converted to $[Mn_3O_4(OH)(bpea)_3](ClO_4)_3$ (**2**) in 90% yield by adding an aqueous solution of $NaClO_4$ to a CH_3CN solution of **1**. Compound **2** crystallizes from $CH_3CN/C_6H_5CH_3$ in the monoclinic space group $P2_1/n$ with a = 10.875 (4) Å, b = 26.074 (9) Å, c = 18.437 (5) Å, β = 103.80 (2)°, V = 5077.2 (6) Å^3, and Z = 4. The structure of **2** consists of three Mn(IV) ions, with two (Mn_b) being coupled together by two doubly-bridging oxo groups (O_b) and the third (Mn_a) being singly-bridged to each Mn_b atom by oxo groups (O_a). Atom Mn_a bears a terminal OH group which is hydrogen bonded to an O_b group. This interaction appears to be in part responsible for a distortion that brings Mn_a out of the plane of the two Mn_b and two O_a atoms. The EPR spectral properties of **2** are consistent with an $S = {}^3/_2$ ground state. Magnetic susceptibility data in the range 6–280 K using an applied magnetic field of 5 kG were also consistent with an $S = {}^3/_2$ ground state and were fit using the Hamiltonian $\mathcal{H} = -2J(\hat{S}_1{\cdot}\hat{S}_2) - 2J'(\hat{S}_1{\cdot}\hat{S}_3 + \hat{S}_2{\cdot}\hat{S}_3)$ ($S_1 = S_2 = S_3 = {}^3/_2$; J = −76 cm^{-1}, J' = −11 cm^{-1}). Both **1** and **2** were further characterized with UV–vis, infrared, and electrochemical measurements. The relationship between **2** and two other species that contain the $\{Mn_3O_4\}^{4+}$ core is discussed. The similarity between the ground spin state variability for synthetic trinuclear manganese oxo complexes and the manganese site in photosystem II is noted.

Introduction

Currently, an abundance of experimental evidence suggests that water oxidation and accompanying dioxygen generation take place in photosynthetic organisms at a polynuclear manganese aggregate within the thylakoid membrane-bound photosystem II oxygen-evolving complex (MnOEC).[2-4] The exact nature of this manganese complex has not been established despite the fact that it has been characterized extensively with a variety of spectroscopic and magnetic techniques.[2,3] X-ray absorption experiments have established the existence of at least two 2.7-Å Mn···Mn contacts within the MnOEC. Attempts to prepare synthetic analogs for the MnOEC have led to the discovery of many interesting polynuclear manganese–oxo species.[5-11] To our knowledge only one of these, $[(Mn_2O_2)_2(tphpn)_2]^{4+}$,[12] faithfully mimics an EPR signal associated with the MnOEC.

A fascinating feature of the PSII manganese aggregate when poised at the so-called Kok S_2 oxidation level is the existence of two distinctly different EPR spectral signatures:[2,3] (i) a signal centered at g = 2 with a minimum of 16 hyperfine components at X-band frequency and (ii) a broad absorption with g_{eff} = 4.1

† Current address: Department of Chemistry, Boston College, Chestnut Hill, MA 02167.

(1) Abbreviations used are as follows: PSII, photosystem II; OEC, oxygen evolving complex; EXAFS, extended X-ray absorption fine structure; EPR, electron paramagnetic resonance; NMR, nuclear magnetic resonance; IR, infrared; bpea, *N,N*-bis(2-pyridylmethyl)ethylamine; tmtacn, *N,N',N''*-trimethyl-1,4,7-triazacyclononane; tacn, 1,4,7-triazacyclononane; $HBpz_3$, hydrotris(pyrazol-1-yl)borate; phen, 1,10-phenanthroline; bpy, 2,2'-bipyridine; tpma, tris(2-pyridylmethyl)amine; pic, picolinic acid; bispicen, *N,N'*-bis(2-pyridylmethyl)-1,2-ethanediamine; tpen, *N,N,N',N'*-tetrakis(2-pyridylmethyl)-1,2-ethanediamine; dmepa, ((6-methyl-2-pyridyl)methyl)(2-(2-pyridylethyl))(2-pyridylmethyl)amine; salpn, 1,3-bis((2-hydroxybenzyl)imino)propane; 5-NO_2-sadpen, bis(3-((2-hydroxy-5-nitrobenzyl)imino)propyl)-methylamine; bispictn, *N,N'*-bis(2-pyridylmethyl)-1,3-propanediamine; bispicbn, *N,N'*-bis(2-pyridylmethyl)-2,3-butanediamine; bispichxn, *N,N'*-bis(2-pyridylmethyl)-1,2-cyclohexanediamine; Fc, ferrocene; TEAP, tetraethylammonium percholorate.

(2) Debus, R. J. *Biochim. Biophys. Acta* (*Reviews in Bioenergetics*), in press.

(3) Brudvig, G. W.; Beck, W. F.; dePaula, J. C. *Annu. Rev. Biophys. Chem.* **1989**, *18*, 25–46.

(4) Govindjee; Coleman, W. *Sci. Am.* **1990**, *262*, 50–58.

(5) Armstrong, W. H. In *Bioinorganic Chemistry of Manganese*; Pecoraro, V. L., Ed.; VCH: New York, 1992; pp 261–286.

0002-7863/92/1514-6398$03.00/0